

We are IntechOpen, the world's leading publisher of Open Access books Built by scientists, for scientists

6,900

Open access books available

186,000

International authors and editors

200M

Downloads

Our authors are among the

154

Countries delivered to

TOP 1%

most cited scientists

12.2%

Contributors from top 500 universities



WEB OF SCIENCE™

Selection of our books indexed in the Book Citation Index
in Web of Science™ Core Collection (BKCI)

Interested in publishing with us?
Contact book.department@intechopen.com

Numbers displayed above are based on latest data collected.
For more information visit www.intechopen.com



Acoustic Emission in Drying Materials

Stefan Jan Kowalski, Jacek Banaszak and
Kinga Rajewska

Additional information is available at the end of the chapter

<http://dx.doi.org/10.5772/54796>

1. Introduction

Drying of wet materials is one of the oldest and most common unit operation found in diverse processes such as those used in the agricultural, ceramic, chemical, food, pharmaceutical, pulp and paper, mineral, polymer, and textile industries. It is also one of the most complex and least understood operations because of the difficulties and deficiencies in mathematical descriptions of the phenomena of simultaneous – and often coupled and multiphase – transport of heat, mass, and momentum in saturated porous materials. Drying is therefore an amalgam of science, technology, and art, or know-how based on extensive experimental observations and operating experience [Strumiłło, 1983; Mujumdar (Ed.), 2007].

Drying processes ought to be appropriately arranged and operated to obtain a high quality dried products, that is, products without excessive deformations, surface cracks, and above all crosswise fractures. A non-uniform moisture distribution in products arising during drying causes a non-uniform material shrinkage and generates stresses, which are responsible for permanent deformations and material fracture. A risk of fracture in drying samples is possible to analyze both theoretically and experimentally. Mechanistic drying models make the basis for numerical simulations of drying kinetics and analysis of the drying induced stresses [Kowalski, 2003]. In this way it is possible to determine the spots, where the drying induced stresses reach maximum and the possibly crack may occur [Kowalski and Rybicki, 2007]. The theoretical predictions are confronted with the experimental data obtained due to application of the acoustic emission method (AE), which enables monitoring *on line* the development of the drying induced fractures caused by stresses [Kowalski et al., 2000].

The acoustic emission method (AE) is a non-destructive method allowing indirect control of micro- and macro-fracture development during drying and above all the identification of the

period and also the place where the fractures start to develop. In this sense the AE is a method that enables control of drying process and help to protect the material against destruction [Kowalski, 2010]. Thus, the EA provides a unique advantage of early detection of subcritical crack growth and recognize when and where the crack is growing. The cracks and deformations arising inside dried materials constitute the AE source. The intensity of AE signals, their number and energy inform about the state and magnitude of stresses [Kowalski, (2002), Kowalski et al., (2004)].

The aim of this chapter is to show the possibly using the AE method to diagnostic purposes of destruction due to monitoring materials subjected to drying. The results of the tests obtained from convective and microwave drying of ceramic and wood materials carried out in the laboratory drier equipped with the acoustic emission set-up constitute the illustrative material of this chapter.

The example under analysis concern cylindrical samples made of kaolin and wood. Based on the mechanistic drying model, the stress distribution in the samples and its evolution in time were determined. In this way the moment at which the stresses reach the critical value causing material damage was appointed [Kowalski et al. 2012]. The system of double coupled differential equations of this model, adopted to the cylindrical geometry, was solved numerically with the help of the finite element (FEM) and the finite difference (FDM) methods. Due to AE method, the number and the energy of AE hits were measured, and the crest value of acoustic waves was appointed, and these data enabled validation of the theoretical predictions. A good adherence of the theoretical and experimental results serves for identification of fractures occurring in materials during drying.

2. The essence of acoustic emission (AE) in drying

2.1. AE descriptors

- Different regimes of compressional acoustic waves propagating through the material from the crack places to the AE detectors attached to the samples, can be identified through the proper choice of the AE descriptors. The descriptors suitable to assessment of mechanical phenomena occurring in drying materials are selected mostly to be: *the number of acoustic emission hits*, *hit rate* (showing the dynamic of the process), *the maximum energy of hits*, and *the crest value* (showing the power of AE signals).
- When applying the AE method to drying processes, a suitable selection of AE descriptors that let to obtain the most useful information about the phenomena occurring in dried materials is an important issue. The parameters characterizing the AE signals that are recorded by the detector inform about intensity and possible size of destruction, and therefore are significant for the precise assessment of the AE occurrence. So, the appointing of the descriptors which qualitatively fit best for description of the AE occurrence is a responsible and difficult task.

- Based on the authors' experience and the performed up to now experiments, it was stated that AE descriptors best reflecting the character of mechanical phenomena occurring in drying materials, are:
- *Hits rate*. This descriptor shows the dynamics of the destruction development (e.g. a rise of temperature drying involves rapid growth of the AE hits rate). Moreover, this descriptor indicates the stages of drying, in which the reduction or increase of the AE activity takes place.
- *The hit of maximum energy*. This descriptor is more useful than that "energy of hits" as it shows the single hit with maximum energy in a given time interval. The descriptor "energy of hits" presents the energy of all hits in a given time interval.
- *Crest value*. This descriptor presents the intensity of hits in time. It is a very significant parameter illustrating the "power" of existing hits.
- *The total number of hits and the total energy of hits*. These parameters show some individual phenomena occurring during drying. Thanks to these descriptors it is possible to distinguish stages of drying in which some irregular changes of the AE energy or the AE hits rate appear. These descriptors point out the critical moments of drying, in which the fracture of drying material may occur.

2.2. Calibration of AE energy

The registered by the equipment AE signals are characterized by two fundamental parameters: the amplitude and the time of signal duration. The relative energy of each signal, called also the acoustic energy of AE signal, is possible to determine integrating the surface under the envelope curve of this signal. It is a relevant characteristics of the magnitude and power of the AE signal source. By application of the AE method to monitoring of drying processes, which are characterized with constant reduction of moisture content (MC) in dried materials, it should be taken into account that the AE energy depends on the material MC. If assume that the sources of AE signals cause cracks of a similar size, however, occurred first in wet material and next in dry one, then, the registered by the equipment AE signals will be different for these two events. This follows from damping of the acoustic waves propagating though a not perfectly elastic material. It is obvious that a more saturated material characterizes with stronger damping properties than an unsaturated one. Therefore, it is essential to take into account the damping effects by analysis of the AE energy descriptors.

It is necessary then to carry out the calibration of the AE energy for each examined material in dependence on its MC. There is a number of calibration methods (Malecki and Ranachowski 1994, Banaszak and Kowalski 2010). Here, the mechanical method is presented, that is, the method of falling ball (Berlinsky at al. 1990, Luong Phong 1994). The calibration was carried out with the use of the equipment presented in figure 1.

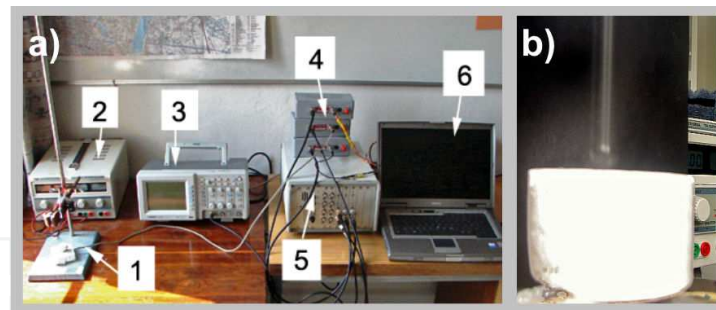


Figure 1. AE energy calibration set-up: a) 1 – the ball's releasing mechanism and AE sensor, 2 – AC power supplier, 3 – oscilloscope, 4 – pre-amplifier, 5 – AE acquisition system AMSY5, 6 – computer, b) impact of dropping ball at the upper kaolin sample surface

A still ball of mass $m = 5.60$ g and diameter $d = 11$ mm was used as a source of acoustic signals having known and constant energy. The ball was planted in the grip with release mechanism, being the electromagnet connected to the power supply adaptor of direct current (2). The ball was situated at height of 10 cm above the upper surface of the sample. The AE sensor (1) was attached to the bottom surface of the sample. The registered AE signals were conveyed through the pre-amplifier (4) to the module unit AMS-5, where they were processed by means of control unit (6). The digital oscilloscope (3) was connected to the system to analyze the course of signal appearance and to assign the level of noise.

The release from the grip ball hit the upper surface of the sample (Fig. 1b) and generated elastic wave, which experienced damping when propagating through the not perfectly elastic sample. After its arriving to the AE sensor, it became converted into the electric signal and next undergone a suitable energetic analysis. Each test was repeated five times for each sample of given MC, and the average value was taken for further considerations. On the basis of those tests the curve of attenuation of the AE energy was determined as a function of the material MC. Figure 2 presents the results of the research carried out for the kaolin and the walnut wood.

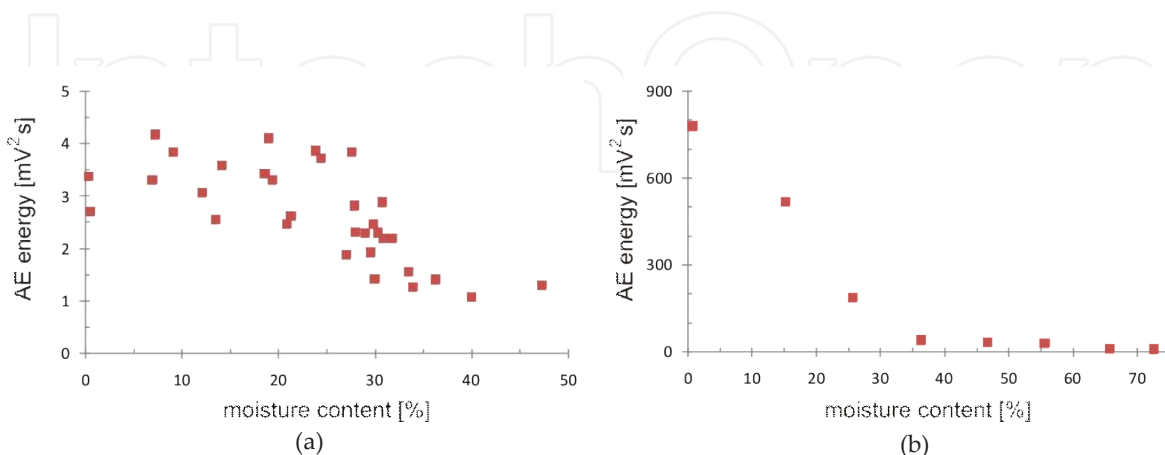


Figure 2. Damping of EA energy in dependence of material MC determined in the test of falling ball: a) kaolin, b) walnut wood

Damping of the AE signal energy depends strictly on the material moisture content. Kaolin material becomes plastic for the moisture content over 27-29% and thus it stronger attenuate the AE signals than that unsaturated one. For the walnut wood the attenuation of acoustic waves becomes very strong for the moisture contents above the fiber saturation point (FSP) (ca. 30%), and there remain on a constant level. Dry wood is a very acoustic material and the energy of AE signal in such a material is weakly attenuated. Alongside with the increase of the MC up to the fiber saturation point the damping of EA waves increases radically. Over this critical MC wood stops to be acoustic material and utters characteristic hollow sounds. It should be noted a very intensive linear drop of energy in the range below the fiber saturation point, what means that wood is a material very sensitive to changeability of the moisture content, for example, music instruments made of wood should be always adjusted to the actual air humidity.

There is a necessity of suitable correction of the energetic values of AE signals received from the measurement set-up, dependent on the actual MC of the material. For this purpose it is necessary to construct the calibration curve of AE energy for the tested material. It can be constructed by the best adjustment of the theoretical curve expressed by the fourth order polynomial to the experimental data. (Fig. 2).

Figure 3 presents the results of measurements of the mean energy of AE events for kaolin and walnut wood during drying with and without taking into account the calibration curve.

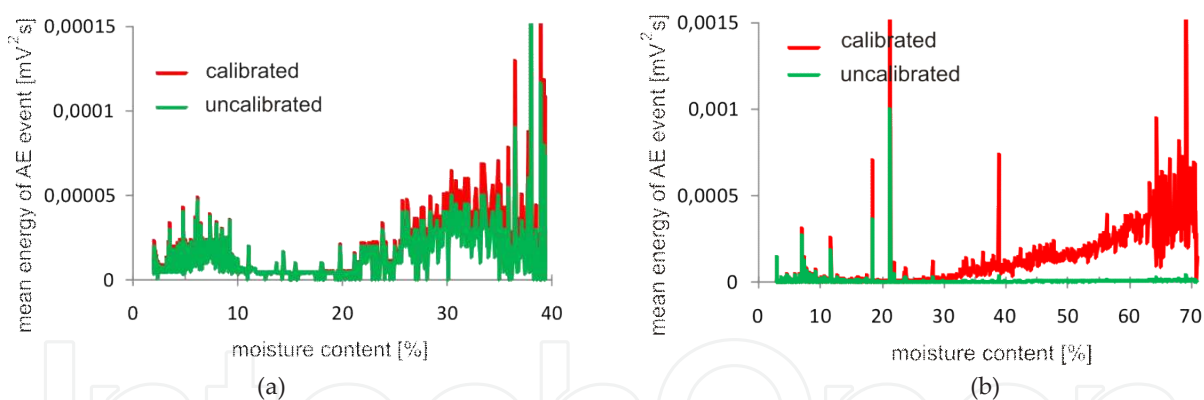


Figure 3. Comparison of mean energy of a AE hits as the function of material MC with and without taking into account of the damping effects during drying: a) kaolin, b) walnut wood

The curve of calibrated AE energy for kaolin has not a significant impact on the final results by the analysis of the AE events. The character of plots with and without taking into account the calibration curve is similar. It follows from insignificant difference in AE signal attenuation for saturated and unsaturated materials. For walnut wood, however, at the beginning of drying (ca. 70% MC) there were registered low energetic AE signals only. High energetic signals appear else by about 20% MC. Taking into consideration the fact that wood strongly attenuates the AE signal with increase MC, then, it can be noticed (Fig. 3b) that the real annotated AE energy, measured with using calibration curve, is significantly higher. It influences then the analysis of AE signals for MC above the fiber saturation point (30%). Some signals arriving to

the AE sensor are high energetic ones even for MC 70% to 60%. The initial high energetic signals for such a high MC originate from sample heating. For example, the AE signal registered for 39% MC originates from a crack in the sample. This AE event could be identified else after taking into account in the analysis the calibration curve presenting the effects of AE energy damping. The other high energetic signals, connected with the successive cracks in the sample, were registered for the sample with MC below the fiber saturation point. They are clearly visible both for the calibrated and not calibrated energy with respect to the material MC.

The presented above results show how important is taking into account the damping of AE signals in studies of drying processes in which the AE method is used for monitoring of the mechanical effects, particularly in wood. Without such an approach a part of the AE signals can be wrongly interpreted, for example, some crack occurrence could not be noticed.

3. Experimental setup equipped with AE measurement instruments

3.1. Scheme of the equipment

The drying tests were realized in the laboratory hybrid drier in the Department of Process Engineering, Institute of Technology and Chemical Engineering, Poznań University of Technology. Presented in this chapter experimental results has been taken for over a decade and according to technical progress our measurement instruments obviously has changed few times during those years. Figure 4 presents the photograph of the latest dryer version equipped with the acoustic emission (AE) system.



Figure 4. Photo of the laboratory hybrid dryer

Figure 5 presents the scheme of the dryer. The cylindrical kaolin or wood samples were placed in the drier chamber on a special ceramic thimble with mandrel embedded on the balance located beyond the chamber. In this way the measurement of the sample weight was possible continuously during all kinds of drying, also during microwave drying. The AE detector was attached either directly to the sample foundation by convective drying or indirectly to the ceramic thimble with mandrel by microwave drying.

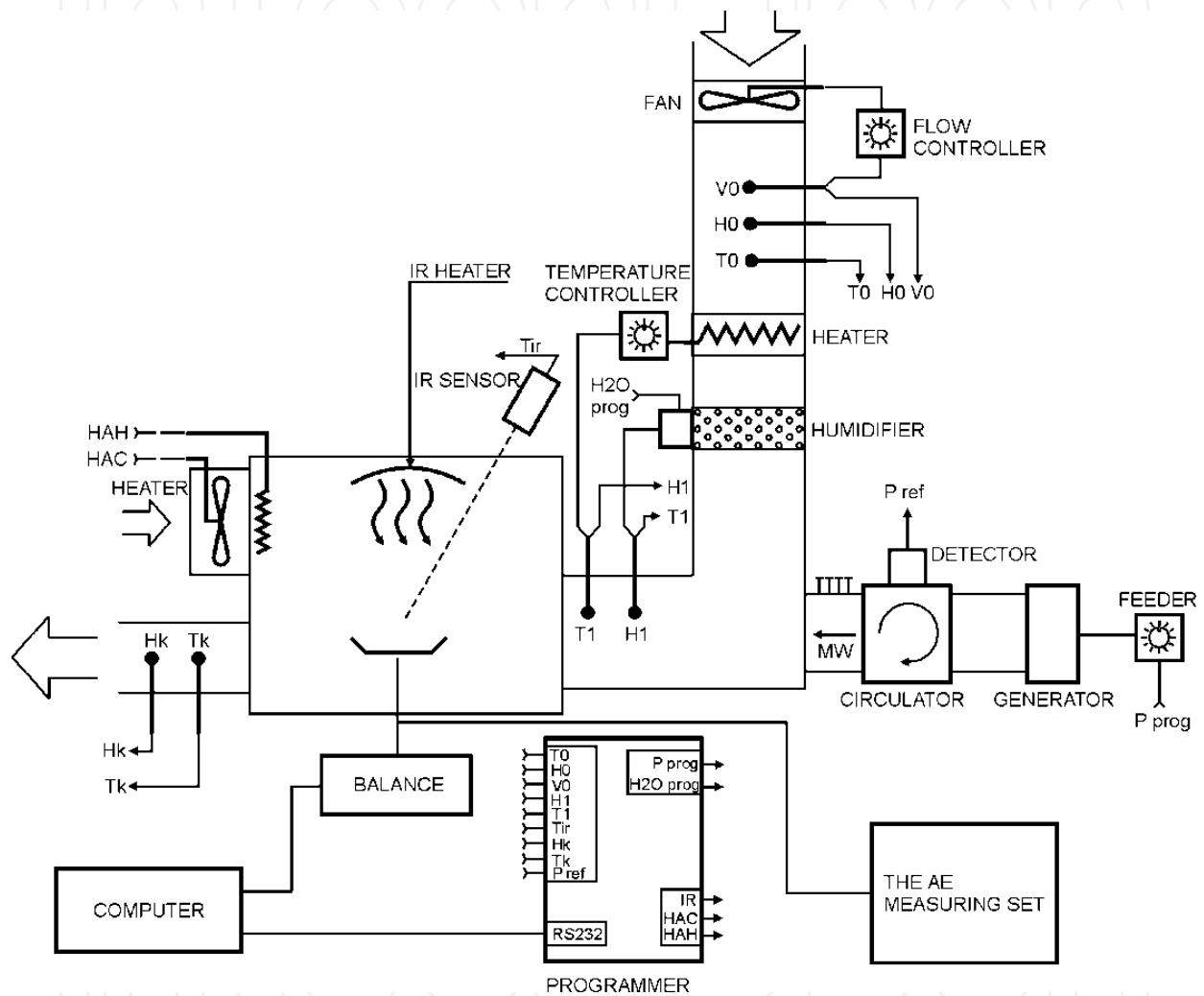


Figure 5. Scheme of the hybrid dryer

The hybrid drier enabled different combination of the three methods of drying: the convective, microwave, and infrared. The drier instrumentation enable programming and control of the velocity and temperature of the air supplied to the drier chamber, control of the microwave power, two-step control of the infrared heater, and the measurement of the sample surface temperature with the help of the optical pyrometer

3.2. Methodology of AE measurement

The AMSY-5 AE system manufactured by Vallen Systeme, GmbH is shown in figure 4. The sample subjected to convective drying was placed on the aluminum plate with fixed piezoelectric sensor. Acoustic signals generated in the drying sample are registered by broad-band transducer. Next the signals were sent via insulated cable to AEP3 preamplifier unit. Preamplifiers were located close to AE sensors. The main task of preamplifier was amplifying and strengthening the signals enough that they could be sent to the distant main measurement unit. The AEP3 unit was equipped with 5 kHz to 1000 kHz filters. The main unit used in the tests had an M6 master unit for up to six AE channels from which three were fully equipped with ASSIP card. This high speed system could store up to 30 000 AE signals per second. The frequency filter inside the unit was used to eliminate noise sources. It can be set up for each channel separately. In our tests the low and high filters in the range from 12 to 850 kHz were applied to collect AE signals from kaolin and wood samples subjected to drying. The filtered AE signals were digitalized in A/D converter and stored in computer memory. The companion notebook PC had a software to control the whole measure system. During the tests the measured data were analyzed online and displayed on computer monitor so that it was possible to recognize the development of defects within the tested object.

4. Materials and conditions for AE appearance

KOC kaolin-clay from the Surmin-Kaolin SA Company, Nowogrodziec, Poland was the material investigated experimentally and theoretically in the drying tests. For this material some characteristic data necessary for numerical calculation of drying kinetics and drying induced stresses were already given by the Surmin-Kaolin SA Company (see Table 1 in Kowalski et al. 2000). The KOC kaolin-clay is widely applied in ceramic industry for manufacturing sanitaryware and tableware. It provides a good strength and plasticity during shaping of the mentioned products and reveals a reduced amount of pyroplastic deformation in the process of their firing.

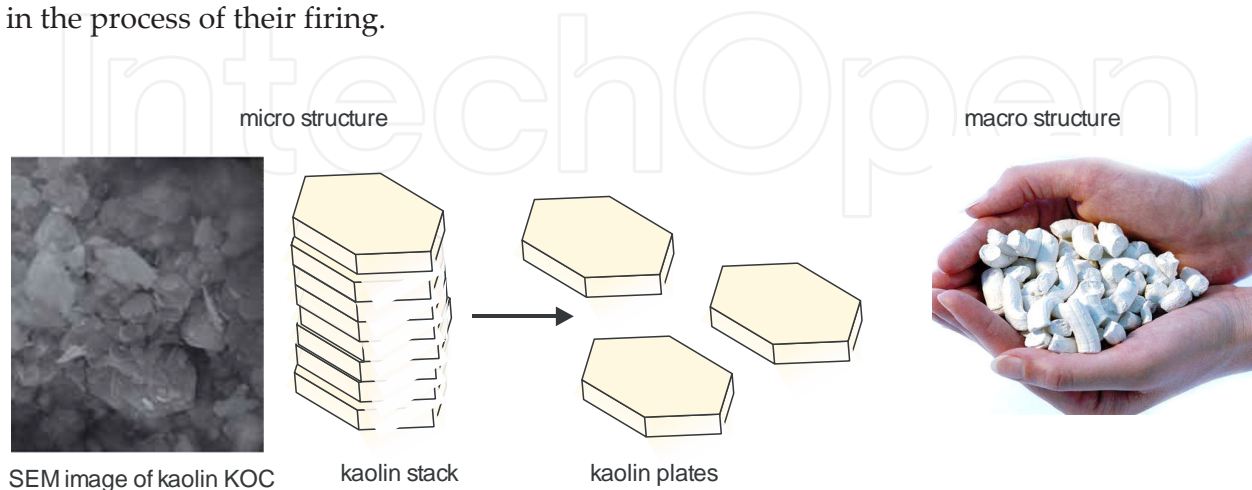


Figure 6. Image of kaolin KOC

The kaolin-clay was delivered in a dry state, and before experiments it was grinded and wetted with a predetermined amount of water and mixed to achieve a greasy paste of initial moisture content (MC) approximately equal to 0.45 [kg water/kg dry kaolin]. The greasy paste was stored and homogenized in a closed box for 48 hours to unify moisture distribution in the whole material. The obtained in such a way soft kaolin-clay mass was used to mold cylindrical samples of 6 cm in diameter and 6 cm height. The cylindrical samples were extruded from a special instrument to preserve their regular shape (Fig. 7a), and samples of such a form were used for drying tests.

Figure 7 shows the shape of kaolin and pine wood samples applied in the studies.

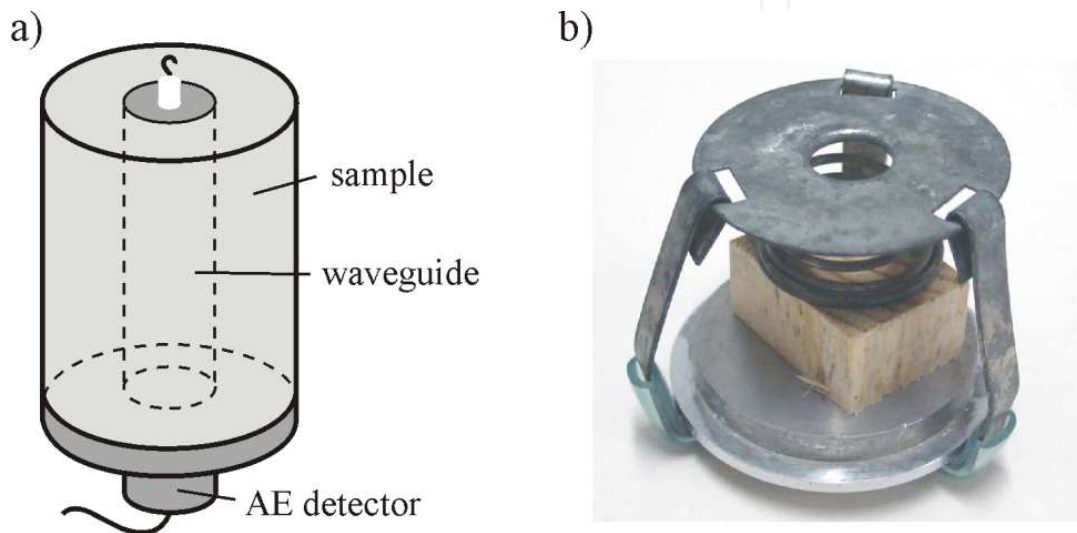


Figure 7. Image of the samples used in drying tests: a) kaolin cylindrical sample with attached AE detector, b) pine wood sample with spring pressed the sample to the AE detector

Samples of the pine wood in the form of cuboid of dimensions about 4×4×2 cm were cut from the blade of the trunk of diameter about 30 cm and keep the symmetry with regard to the axis of the core. The walnut samples were of cylindrical form with height about 26 ÷ 27 mm and the diameter about 44 ± 2 mm. These samples were cut out from walnut branches deprived of defects in the structure. They contained 5 annual growth rings on average. The samples were placed on the aluminum support to which they were pressed with the springs to get a better contact with the AE sensor. The initial humidity of pine wood samples was about 117% and walnut samples about 85%. The samples prepared in this way were used to convective and microwave drying tests in the laboratory dryer presented above.

5. Examples of AE in drying materials

5.1. Convective drying of ceramic-like materials

One of the goals of the realized tests was to interpret the AE signals that may occur during drying of kaolin-clay (Fig. 8). The first (I) characteristic group of AE signals appears at the

beginning of drying process, the second (II) one in the period when the surface layer intensively shrinks, and third (III) one is noticeable sometimes in the final stage of drying and identified as being generated by the reversed stresses.

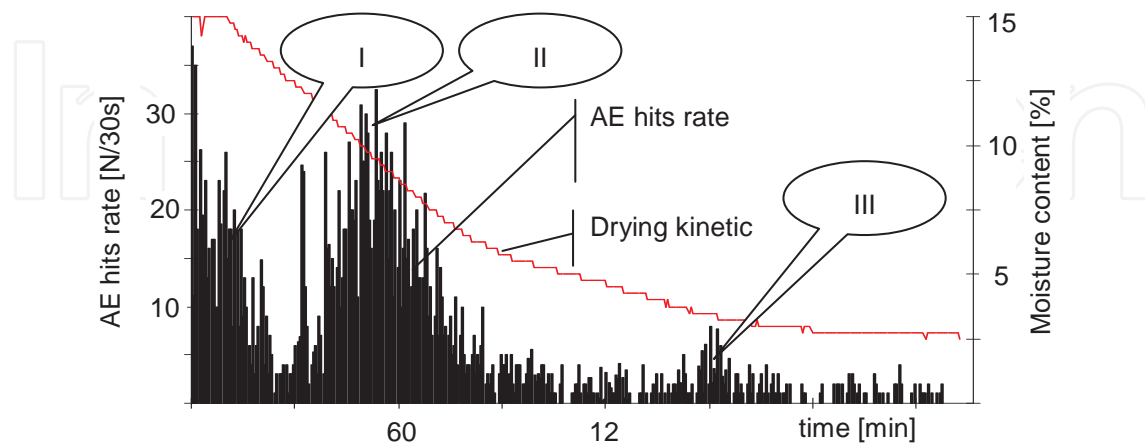


Figure 8. AE signals and the curve of drying

As the drying body is almost fully saturated at the initial stage of drying, the number and the maximum value of AE signals in the heating period (I) is proportional to temperature of the drying process. At this stage of drying, the thermal stresses dominate in the clay sample which are rather not so much meaningful. Unfortunately, at the initial stage of drying some of AE signals come from heating aluminium probe and the AE sensor. It is hard to decide which AE signals in this stage of drying are from the investigated kaolin-clay sample and which from other sources. In tests with lower process temperatures the first maximum was also lower.

The second group of AE signals is evidenced at the end of the constant drying period (II). Their number is the highest of the whole drying process. The reason for appearance of these signals can be explained by the tensional stresses that arise at the external layers of the cylinder as a result of shrinkage. The surface of the body becomes more and more dry while its core is kept still wet. The first cracks on the external surface of the cylinder are observed when the local stress reaches the yield strength or the strain exceeds the allowable ultimate limit.

The third (III) maximum of AE signals is rather of small or moderate magnitude and depends on drying conditions. It was stated that this maximum exists usually for high temperature or low humidity of the drying medium. It holds for porous materials revealing inelastic properties (e.g. wet wood, clay, kaolin), and can be explained as follows: at the beginning of drying, the external layers are stressed in tension and the core in compression. Inelastic strains occur both in the surface layer and in the wet core. Later, under a surface layer with reduced shrinkage, the core dries and attempts to shrink causing the stress state to reverse. These new induced tensional stresses in the core cause fracture of a brittle (almost dry) structure, in what follows generate the acoustic signals.

Fig. 9 presents the rate of AE hits for the five different temperatures of drying. It is seen that for the conditions of high drying rates created by high temperatures, the rate of AE hits achieve higher values than for lower temperatures. That high active emission of AE signals has a reflection in the drying induced stresses.

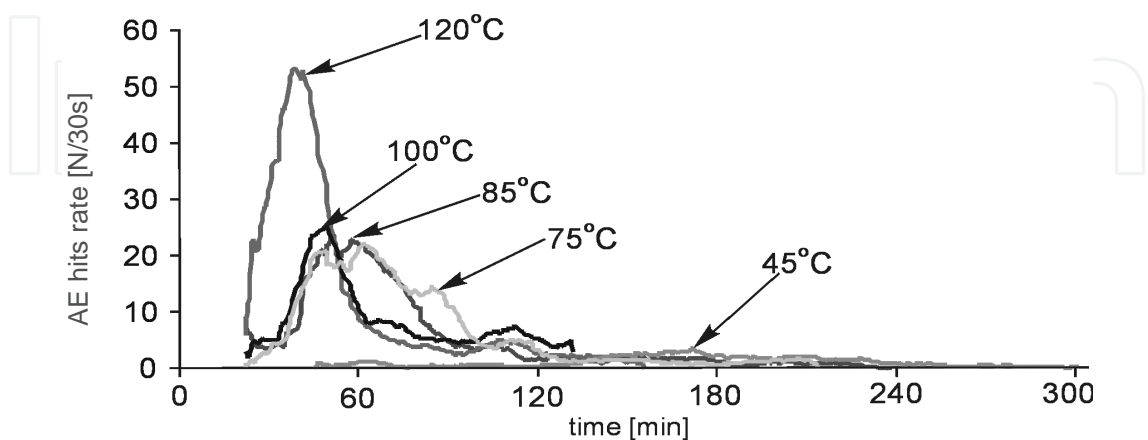


Figure 9. The rate of AE hits during drying at different temperatures

Note that the highest peak of the AE hits, which correspond to temperature 120°C, appears earlier than the lower peaks corresponding to the lower drying temperatures. The primary peak of AE hits appeared in 50 min of drying time, that is, when the tensional stresses at the cylinder surface reached maximum. The secondary peak is visible about 110 min drying time for temperature 120°C. In this time the core of the body starts to dry. The wet core wants to shrink but the surface layer is not able to deform itself because it is almost dry. So, in these circumstances the tensional stresses arise in a core. The secondary maximum is, of course, much lower than the first one.

Another AE descriptor termed *the total energy* is useful in analysis of fracture phenomenon by drying. It measures successively the total energy released during the whole process of drying. Figure 10 presents the rate of AE hits and the curve of total energy versus time.

The curve of summarized in time acoustic energy released during drying can deliver essential information on fracture dimension occurring in the investigated body. A highly fractured material is qualified as a bad quality one. The descriptor of total energy released may serve as an indicator, whether the dried product is of good or bad quality at the end-state. Strong cracks of body structure release high energetic EA signals. The high or medium energetic signals are evidenced in figure 10 as the strait upright lines. In some cases, the high energetic signals denote macro-cracks or splits that are visible on the sample surface. Taking into considerations the above presented curve of total energy one can state that it represents a dried product of bad quality.

The strength of material with damaged structure is impaired. Often a number of internal small micro-cracks arising during drying may nucleate and create macro-cracks during utilization

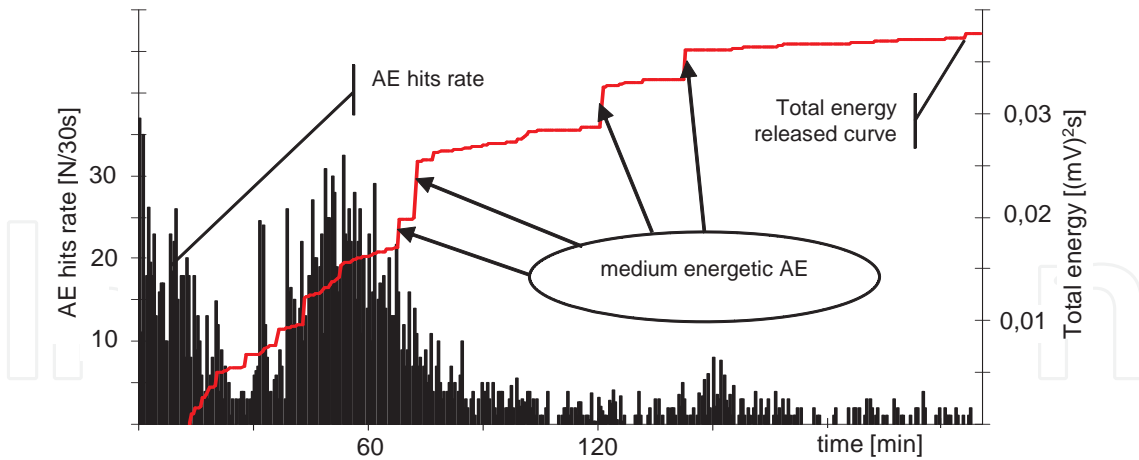


Figure 10. Total energy of AE signals released during drying

of dry products, so that an unpredictable total damage of the body may take place in any time after drying.

The reason for fracture of materials under drying results mostly from not proper drying conditions (e.g. too high temperature or too low drying medium humidity). By optimal drying process the high energetic AE signals ought to be eliminated or minimized. The majority of registered AE signals ought to be low energetic (horizontal or almost horizontal lines in figure 10). Low energetic AE signals mean lack of destruction in dried products.

Figure 11 shows several curves of total EA energy released from kaolin cylinders during drying at different temperatures. Each EA signal carries a certain portion of energy. The flat horizontal lines represent the low energetic signals. Hits of high energy create sudden vertical lines as, for example, those visible on the energy curves obtained for drying at temperatures 100 and 120°C. These very energetic signals are generated by strong material cracks.

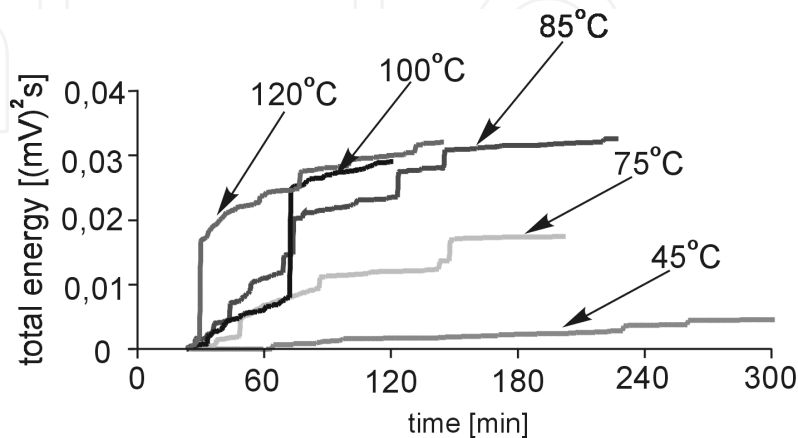


Figure 11. Total energy of hits during drying process for various conditions

Analysing figure 11 one can see the differences in released energy for different drying conditions. The curve of 45 °C, being almost horizontal, represents low energetic AE signals. It means that drying at this temperature is unpropitious for creation of material fracture, so the manufactured product is of good quality and without residual stresses. Unfortunately, drying at such a low temperature takes a long time and is unsatisfactory from the economic point of view.

The total energy curve for drying at 75°C looks a little different from that of 45°C. It contains a greater number of signals in the time period from 40 to 100 min but these signals are not so much energetic either, some of them might be generated by invisible micro-cracks. This curve is slightly inclined upwards.

The next curve (85°C) has similar character as that of 75°C one, however, represents more energetic signals. The energy released here is much higher than that represented by the two previous curves. The dried product at this temperature may have a number of micro-cracks that can expand into visible cracks under the action of residual stresses.

The most energetic AE signals are represented by the curves characterizing severe drying conditions (100°C and 120°C). So, high temperatures together with low humidity of the drying medium (air) are propitious to high drying rate. This produces quickly dry and brittle surface layers while the wet core becomes still wet and deformable. The drying induced stresses cause damage of the fragile surface.

5.2. Microwave drying of ceramic-like materials

Figure 12 presents the photographs of the cylindrical samples after microwave drying with 300 W of the microwave power (MWP). The damage of the cylinder is occurred in its center and looks like an explosion caused by a high vapor pressure inside the cylinder due to intensive phase transitions of water into vapor. This proofs that by microwave heating the highest temperature arises inside the material. It is confirmed by the picture presented in figure 12c made with infrared (IR) camera (Flir therma-cam B2).

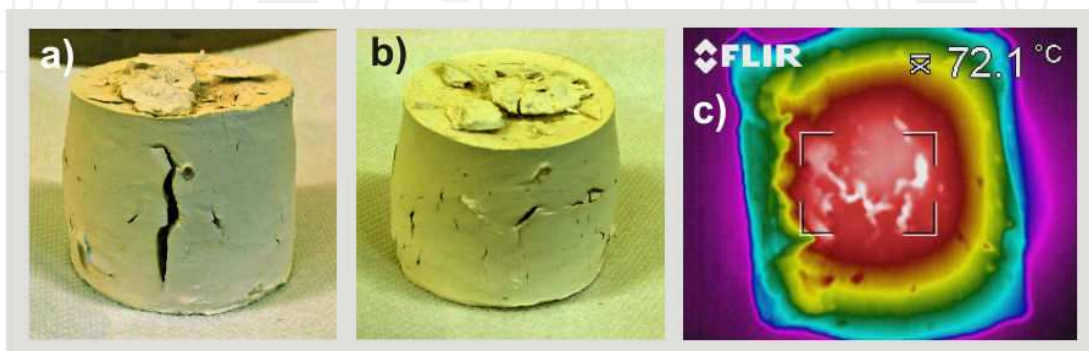


Figure 12. Kaolin sample subjected to 300 W MWP a) front view, b) rear view, c) IR camera picture of temperature distribution in the sample longitudinal cross-section

The sample subjected to 300 W of MWP has a huge vertical slit, almost 3 cm long and 2.5 cm deep (Fig. 12a). It was caused by the explosion after 20 min of drying time. The barrel shape of the samples is very clearly visible in both figures 12a and 12b. The picture of temperature distribution in the sample longitudinal cross-section (Fig. 12c) shows that the temperature reached about 90°C in some hot spots, although the mean temperature in the central part was about 72°C. This indicates the existence of places where the water was rapidly changed into vapor. The rapidly increased vapor pressure created the big slit, so that the water vapor had found the way out.

Figure 13 presents AE signals acquired during microwave drying of kaolin cylinders.

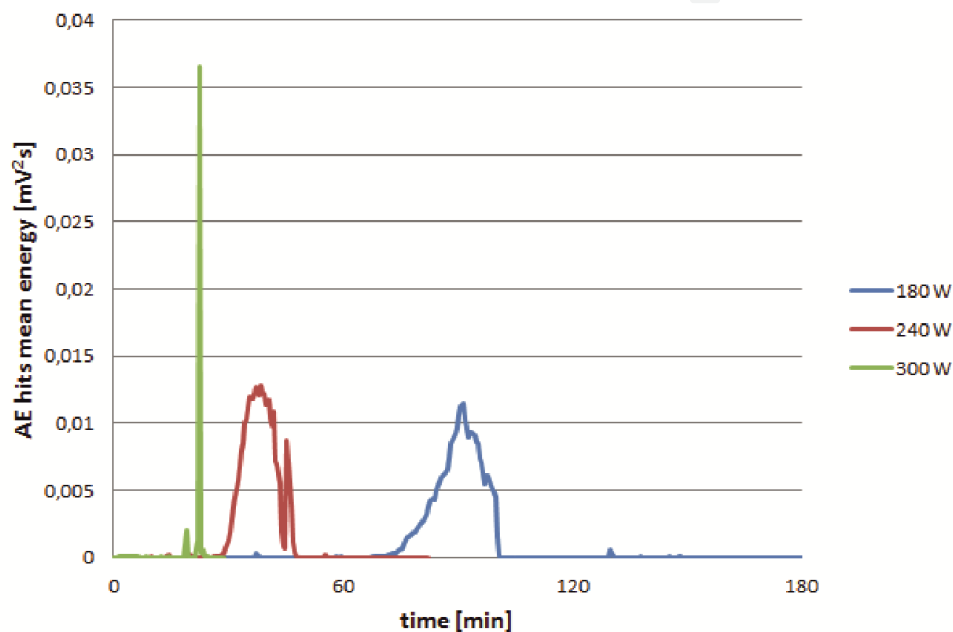


Figure 13. AE hits mean energy acquired during microwave drying of kaolin cylinders

For 300W of MWP the huge acoustic energy wave was generated during the explosion. It is visible in figure 13 as a high single signal at 20 minutes of drying. Drying with lower MWP (180 W and 240 W) induces signals of lower AE energy.

The number of AE signals induced during microwave drying depends on the MWP (Fig. 14). By lower MWP the number of AE signals is greater, but they are of lower energy than those of higher MWP.

The destruction of samples raised by microwave drying proceeds mainly in the second drying rate stage, except the one dried in 300W MWP. For samples dried in 180 W and 240W MWP- s the destruction was observed as step by step splitting small parts (Fig. 15).

The convective and microwave drying methods differ from each other in the way of heat supply. By convective drying the heat is delivered from the surroundings through the material surface from the hot air of temperature higher than the temperature of drying material. By microwave drying on the other hand the heat is generated volumetrically as a result of the

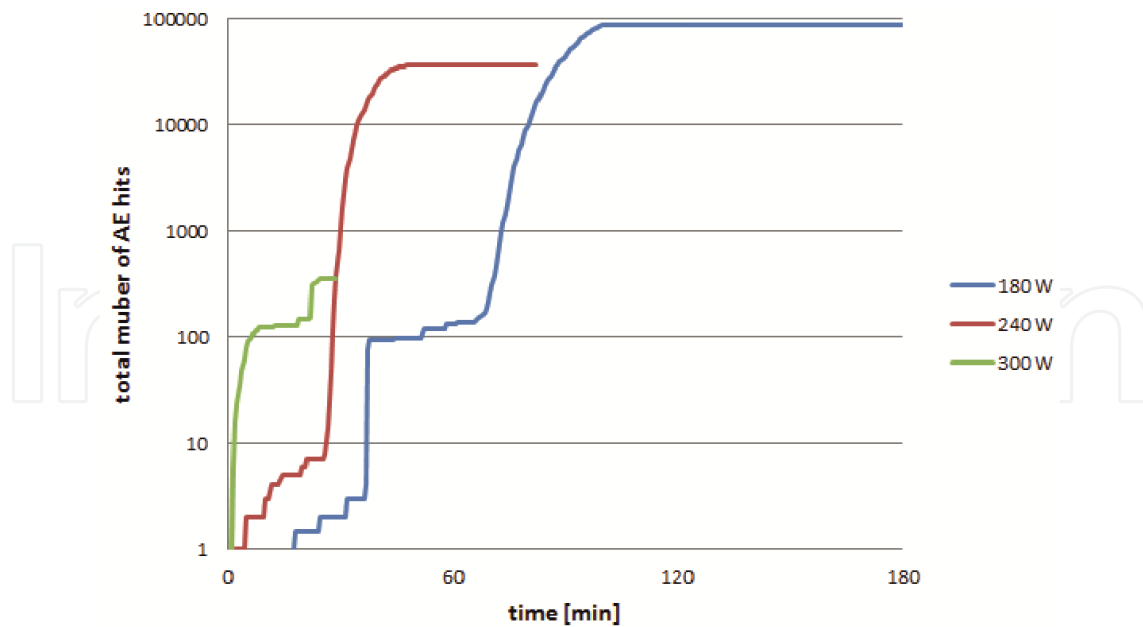


Figure 14. AE results for microwave drying of kaolin: the total number of AE hits

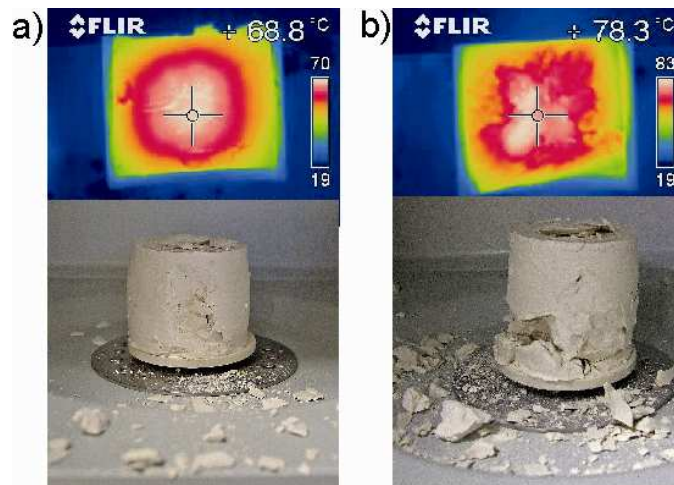


Figure 15. The kaolin sample dried in microwave oven by 240 W MWP

dispersion of the high-frequency monochrome waves of the order 2.45 GHz. The microwave power is absorbed mainly by the water present in the material pores.

The different ways of heat supply affects the directions of heat and mass fluxes. During the convective drying the heat flux is in opposite direction to the mass flux, and this causes a decrease of moisture removal, what is favorable to non-uniform distribution of the moisture inside the material. Such a negative thermodiffusive effect not appears or is minimal in microwave drying by which the heat flux coincides with the mass flux. The interior of the material usually has the temperature higher than the surroundings. The moisture distribution

in the material in this case is more uniform than during the convective drying. So the drying induced stresses should be smaller. Diagrams get from measurements of total numbers of AE signals and the AE energy confirm this prediction.

Figure 16 presents the AE hits in kaolin sample dried convectively. It appears from the presented diagrams that the maximum number of AE signals was occurred in the middle of the constant drying rate period (CDRP).

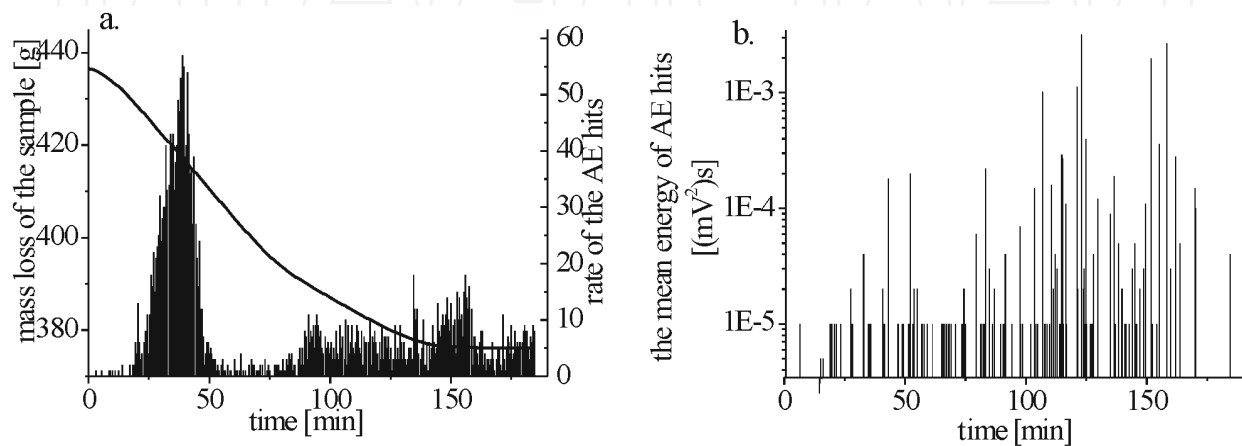


Figure 16. The AE hits for convective drying of kaolin sample: a) drying curve and AE hits rate, b) mean energy of AE hits

Kaolin clay sustains the greatest shrinkage in the initial period of drying (15–90 min). External layers of the cylindrical sample are dried first and shrink generating stresses and cracks, which is manifested by an increased number of AE signals. The density of these signals decreases with the course of drying, however, their energy becomes more and more greater. Figures 16a presents the rate of AE hits and 16b the mean energy of AE hits. One can see that the initial great number of hits is of relatively low energy but the subsequent ones revealed much bigger

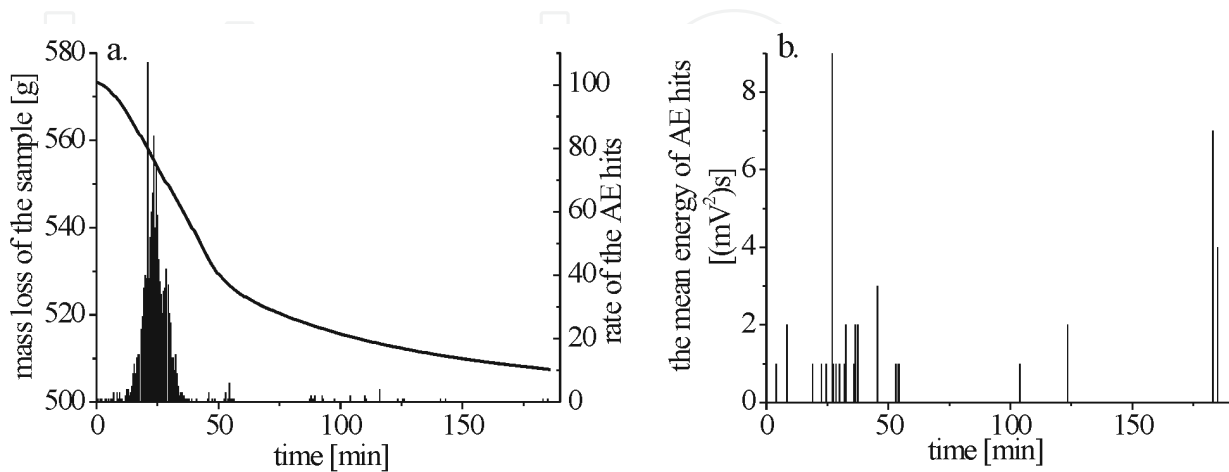


Figure 17. The AE hits by microwave drying of kaolin sample: a) drying curve and AE hits rate, b) mean energy of AE hits

energy. In the latter cases a number of distinct scratches was visible on the surface of dried samples and in some cases even micro and macro cracks were formed, particularly by drying in more severe drying conditions.

Figure 17 presents the AE hits in a kaolin sample that occurred by microwave drying. In the case of microwave drying one can see that both the number of AE hits (Fig. 17a) and the emitted AE energy (Fig. 17b) are much lower in comparison to the convective drying. The lower number of AE hits in microwave drying can be justified by the coincidence of the heat and mass fluxes and thus more uniform distribution of the moisture through the material in this kind of drying, which consequently resulted in reduction of stresses. It is important that a significant increase of drying rate was noticed by microwave drying. The CDRP amounted only from 10 to 70 min (Fig. 17a), dependent on MWP.

5.3. Convective drying of wood

Drying of pine wood samples was conducted at three different temperatures: 60, 80 and 100°C. Figure 18 presents the rate of AE hits, i.e. the density of AE signals per a time interval (e.g. 30 s) (Fig. 18a), and the drying curves (Fig. 18b), for different drying temperatures.

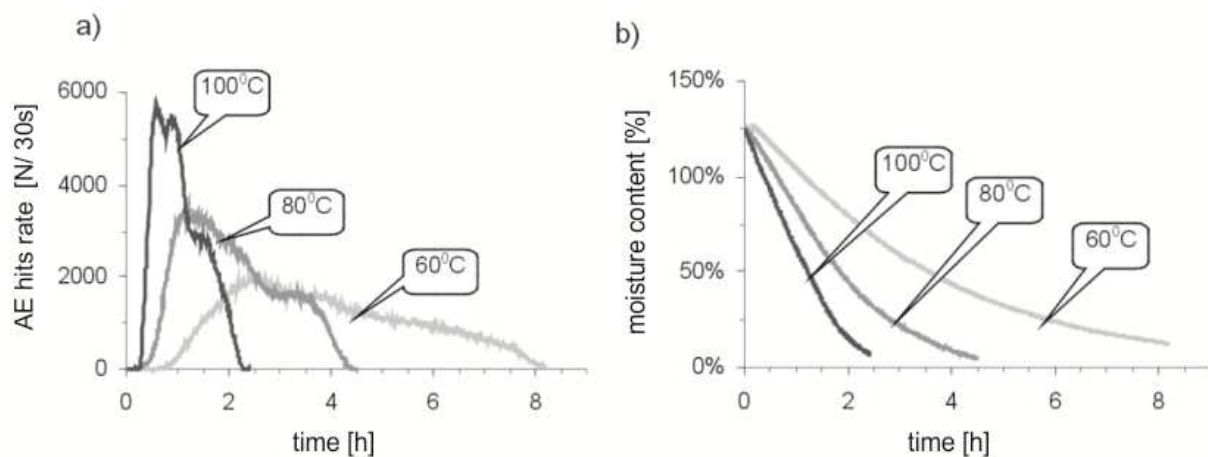


Figure 18. Results of pine wood drying: a) the rate of AE hits, b) drying curves

One can state based on the experimental results that the rate of AE hits in drying wood depends on the number and size of fractures occurred in wood samples. The shrinkage of wood begins at the moment, when the MC reaches the fiber saturation point (FSP) (c.a. 30%). In the initial drying period, when the MC in wood is higher than FSP, the AE activity is insignificant. Only when MC in the surface layers drops below FSP, and the MC inside the samples exceeds this value, the AE start to reveal greater activity, in particular for high drying temperatures. The considerable increase of the rate of AE hits corresponds then with drying stresses and cracks of different sizes, which generate acoustic wave.

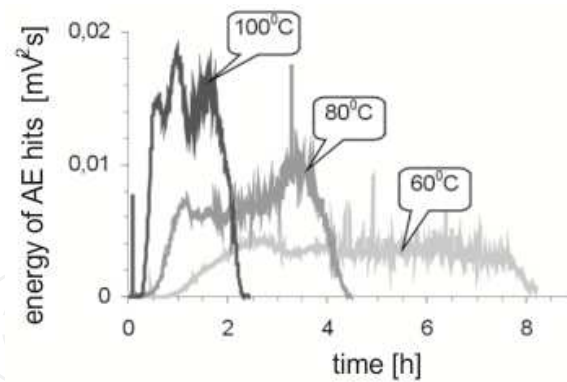


Figure 19. The energy of AE hits for pine wood sample dried at various temperatures

Figure 19 shows the energy of AE hits for pine wood for different drying temperatures. The graphs presented in this figure, and in particular this referring to drying at temperature 100°C, point out a danger of wood destruction at the moment when the AE energy reaches maximum.

As the plots in figure 19 show, the rate of AE hits grow rapidly at the beginning but after some time they decrease also quite rapidly. The rate of AE hits decreases in the period that refers to drying of the sample core, however, the emitted AE energy stays on the same level or even grows, as it is seen on the graph for 80°C. Incurred earlier micro-cracks start expanding and linking. A danger of wood destruction could be then even greater than in the initial period, because of increase of the summarized energy of AE signals. Dried wood becomes more and more rigid and the risk of the brittle cracking becomes more and more probable. Observation of the mean energy of AE hits presented in figure 20 confirms it.

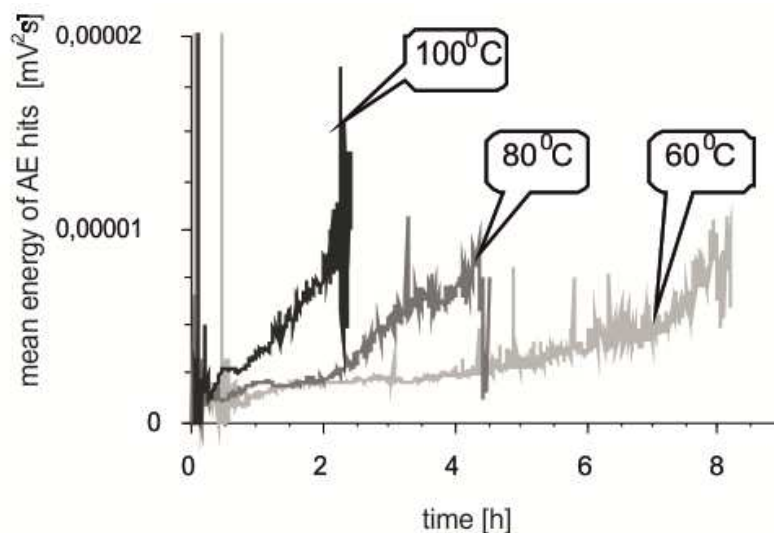


Figure 20. The mean energy of AE hits

The energy is released up to the end of drying process. Incurred earlier micro-cracks grow further. The mean energy of the AE hits is a measure of the progressing decomposition of wood. It is bigger for higher temperatures of the drying medium. However, in the conducted series of drying tests in no case occurred a visible crack of dried sample. This fact is evidenced on the curves of total energy presented in figure 21, that is, the energy summed up during the whole course of drying.

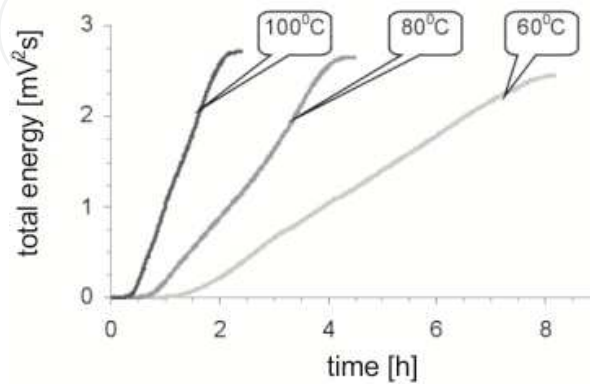


Figure 21. The total energy of AE hits for the whole drying process

One can see that the curves of total energy are growing smoothly, that is, without violent jumps. Violent jumps on graphs of total energy indicate just fractures visible even with a naked eye.

5.4. The phenomenon of stress reverse

The phenomenon of stress reverse results from a constrained shrinkage in dried material. It can happen when the surface of material becomes deformed permanently due to intensive shrinkage. The stresses arose on the surface are tensional and in the material interior compressive ones. When the drying is progressing deeper into the material and its core starts to shrink but is hindered by the surface shell previously stretched in a permanent way, then the stress on the surface becomes compressive and that in the material interior tensional, so thus the stress reverse take place.

Modeling of the stress reverse phenomenon requires taking into account inelastic properties of the materials. This issue was already considered in the work by [Kowalski, 2001, 2002; Banaszak and Kowalski, 2002; Kowalski and Rajewska, 2002; Kowalski et al., 2002].

Figure 22 shows the time evolution of the circumferential stresses distributed in the cylindrical kaolin sample dried convectively by the assumption that kaolin is viscoelastic and obey Maxwell model [Kowalski, 2001, 2002; Kowalski and Rajewska, 2002].

We can see that the circumferential stresses are compressive in the core and tensional in the boundary layer at the beginning and reversibly signed at the end of the drying process. We suppose that the tensional stresses in the core of the cylinder may cause structural fracture and thus the emission of the third group of acoustic signals at the final stage of drying.

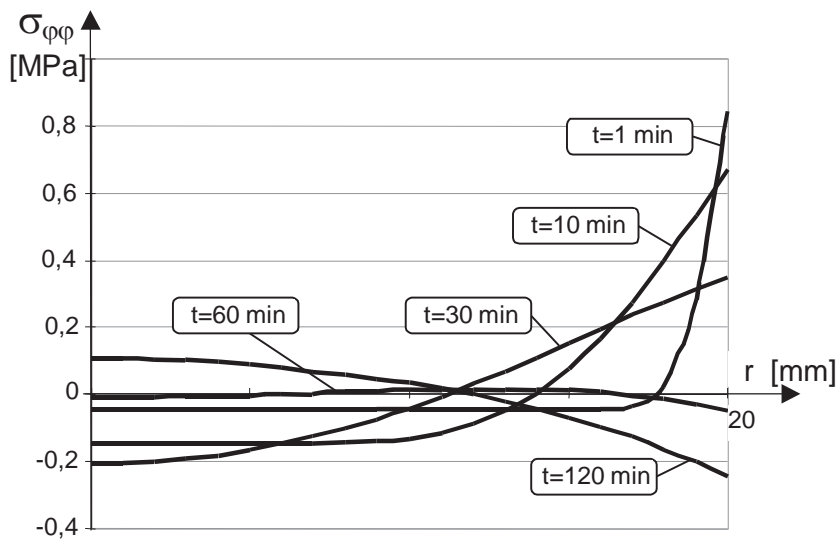


Figure 22. The evolution of circumferential stresses in kaolin cylinder dried convectively

Figure 23 shows the evolution of circumferential stresses in wooden cylinder (birch) dried convectively [Kowalski et al., 2002]. Here the Maxwell model was used for wood.

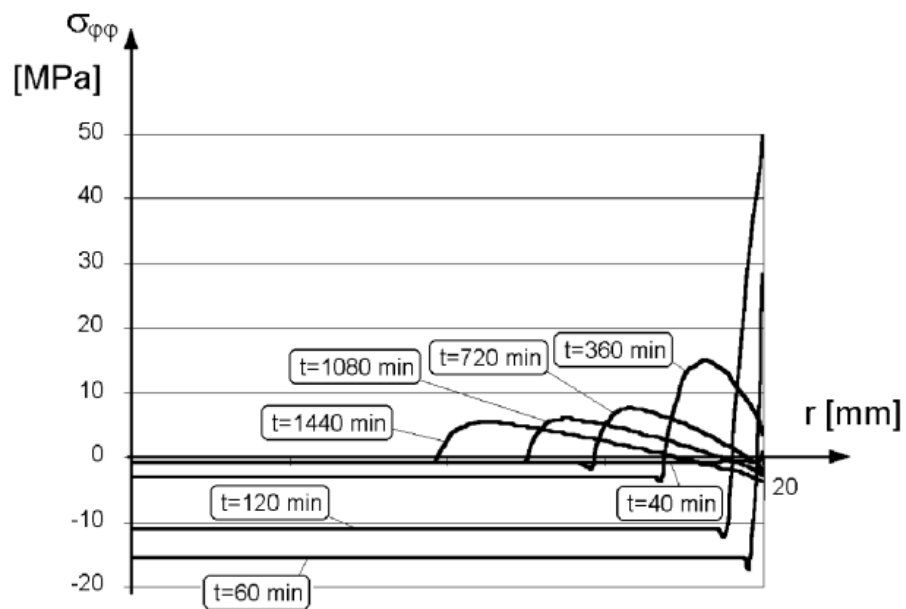


Figure 23. The evolution of circumferential stresses in wood cylinder dried convectively

At the first stage of drying the stresses for the viscoelastic model run in a similar way as for the elastic model. After some time, however, when the dry zone extends deeper towards the wet core, the circumferential stresses start to change their sign at the boundary from tensional to compressive. Note that the maximum value of the tensional circumferential stresses is moving during drying from the boundary surface towards the interior of the cylinder.

Figure 24 shows the evolution of the number of AE hits in time during convective drying of kaolin sample. The plot of the number of AE hits is confronted with the curves presented the circumferential stresses determined on the basis of elastic Hooke model (dashed line) and viscoelastic Maxwell (solid line).

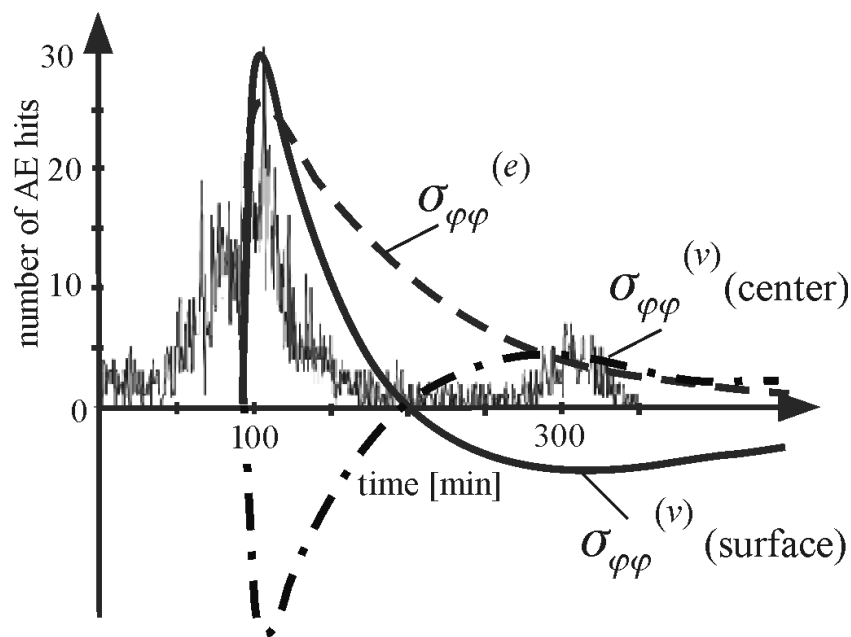


Figure 24. Hits rate and the theoretical curve of circumferential stresses as a function of time

As it is seen from figure 24, Hooke model does not reflect the occurrence of stress reverse. It demonstrates only the compliance of the first maximum of stresses with the increased AE activity. The consideration allow us to appreciate the meaning of the mathematical model adequacy for the description of the mechanical phenomena by drying of wet materials. The experimentally observed enhanced emission of acoustic signals, betoken the enhanced destruction of the material at the final stage of drying. Using the elastic model one obtains the stress development, which rises from the beginning, then reaches a maximum at point in time, and next, as the process proceeds further, disappears totally. Otherwise, the model that takes into account the permanent deformations of the dried material, allows us as in the case of viscoelastic model to observe the stress reverse, and in particular the appearance of tensional stresses inside the dried material at the final stage of drying. The tensional stresses in the core at the final stage of drying cause an increase of AE signals, which is visible in figure 24.

6. Control of material damage with the help of AE

6.1. Avoiding material fractures through changes drying conditions

The non-stationary (intermittent) convective drying denotes drying with different drying rates in several periods. The results of the drying studies presented in this chapter allows to state that the intermittent drying can be recommended above all to drying of materials, which have a tendency to cracking during drying as, for example, ceramics and wood. Through changes of drying conditions in the right moments one can avoid material fracture and thus preserve a good quality of dried products. Thus, one can state that intermittent drying positively influences the quality of the dried materials without significant extension of the drying time.

In these considerations the intermittent drying was realized through periodically changing both temperature and humidity of drying air. The results of intermittent drying are compared with adequate processes of stationary drying to show the profits resulting from the former.

Apart from the visual assessment of the quality of dried products, the acoustic emission (AE) method was applied for monitoring of the micro- and macro- cracks developed during drying [Kowalski and Pawłowski, 2010]. In those studies it was measured the total number of AE hits and the total amount of AE energy emitted. The descriptor of total AE energy is the sum of energy of all acoustic signals emitted by the dried sample from the beginning to the end of drying. It denotes the energy released due to material cracking. These descriptors show the moment at which the AE becomes intensive and how big is the AE intensity. Knowing these descriptors, one can assess the intensity of micro- and macro- cracks that arise in dried materials as well as their magnitude. The "intensity" quantifies the number of cracks per 30 s intervals or the total number of cracks in the whole process. The crack "magnitude" is evidenced as the vertical straight line on the descriptor of total AE energy curve. In this way we can estimate the degree of destruction and how fast the destruction advances in dried materials.

Figure 25 presents the total number of AE hits and the total AE energy emitted during stationary drying of the kaolin cylindrical sample at temperature 100 °C.

The plots in figure 25 show a continuous increase of the number of AE hits and the AE energy. The flatness on the energy plot that begins at about 100 min of drying follows from the release of the elastic energy accumulated in the stressed material due to material fracture, and in this way a reduction of the stress state occurs.

Figure 26 presents the total number of AE hits and the total AE energy emitted from the cylindrical sample during drying with periodically changing temperature between 50 and 100 °C in the falling drying rate period (FDRP).

Note that the total number of AE hits and the total AE energy emitted during drying with periodically changing temperature is less than those in stationary drying. The plots in figure 26 are not so smooth as those in figure 25, which follows from the variable air temperature, and strictly, by switching off and on the air heater and cooler.

Figure 27 presents the total number of AE hits and the total AE energy emitted during drying with variable air humidity. The number of emitted AE hits and the total AE energy in this kind

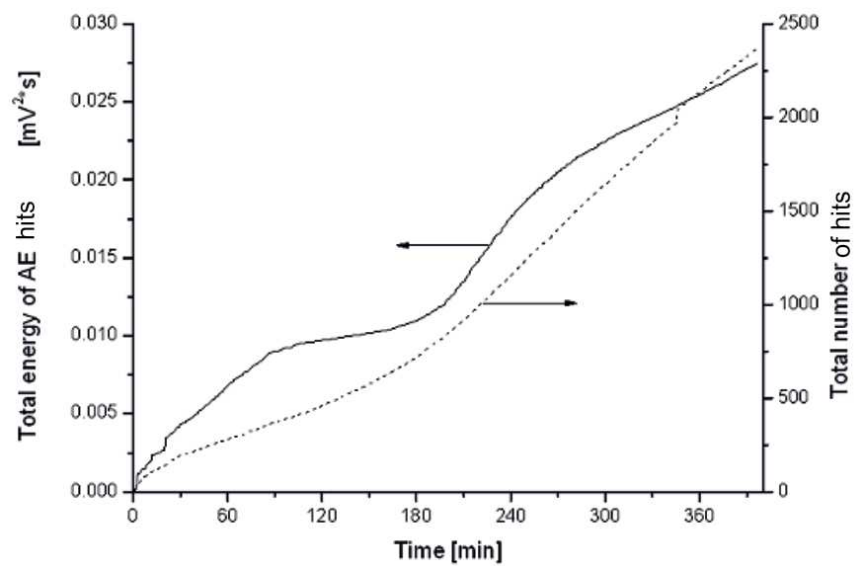


Figure 25. Total number of AE hits and total AE energy in stationary drying of cylindrical kaolin sample at 100°C

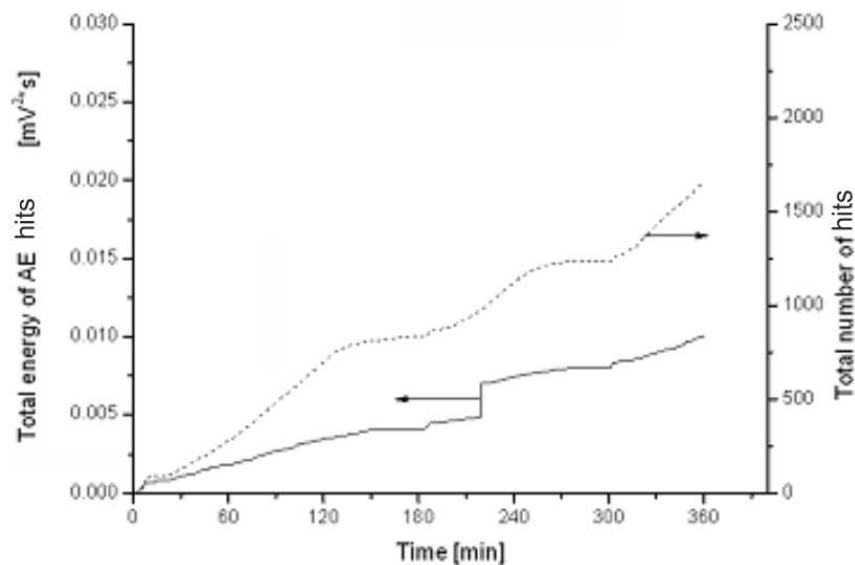


Figure 26. Total number of AE hits and total AE energy by convective drying of kaolin cylindrical sample at periodically changing temperature between 50 °C and 100 °C

of drying is lesser than those during stationary drying and also lesser than during drying with variable temperature.

The humidification of air in the chamber dryer caused the plots of acoustic emission to be very rugged. Nevertheless, we can state that drying in intermittent conditions accomplished through periodically changing temperature and air humidity is accompanied by a smaller number of AE signals and smaller value of AE energy. This denotes less micro- and macro-cracks in dried material and simultaneously better quality of dried products.

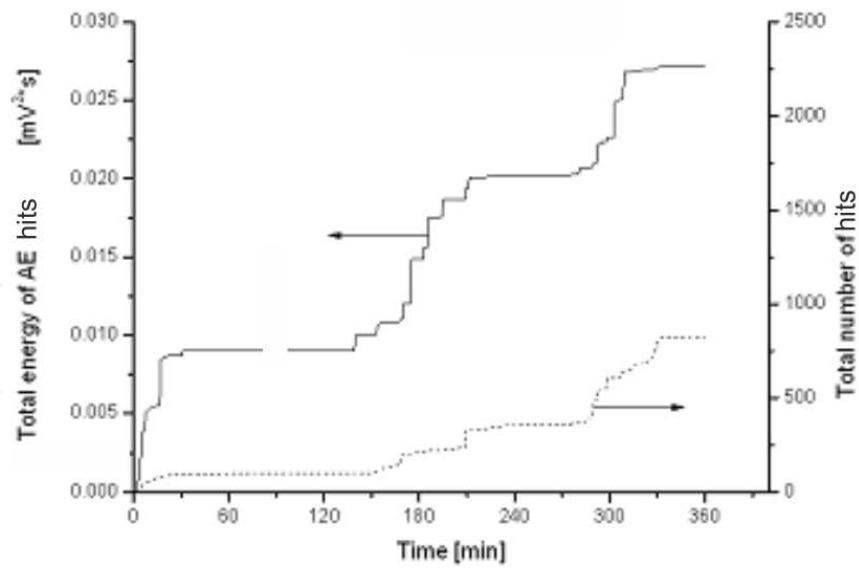


Figure 27. Total number of AE hits and total AE energy by convective drying of kaolin cylindrical sample at periodically changing air humidity between 4 % and 60 ÷ 80 %

6.2. Reduction of material fractures through surfactant application

In order to improve moisture transport inside the dried body, and thus to assure more uniform distribution of moisture in the material and thus avoid its cracking, the authors proposed wetting the raw kaolin-clay with water containing surface active agents (surfactants). These agents have the ability to stimulate the surface tension between water and the pore walls and thus to improve moisture transport inside the material [Cottrell, 1970; Wert & Thomson, 1974].

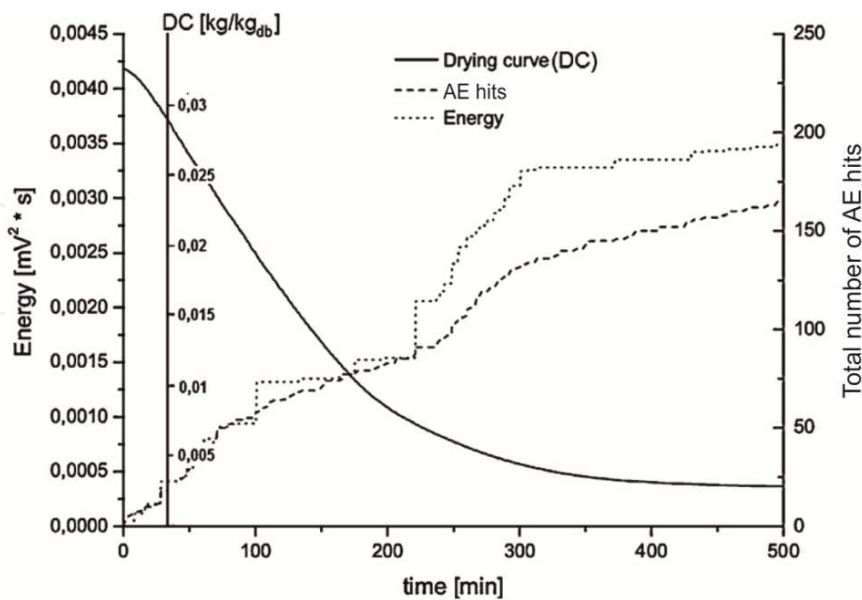


Figure 28. Drying curve, total AE energy and total number of AE hits in clay samples saturated with pure water of clay samples at air temperature 120 °C

Figure 28 presents the typical drying curve of clay samples with the CDRP (0 – 180 min) and the FDRP (180 – 400 min), and the descriptors of total AE energy and total number of AE signals emitted during drying of clay saturated with pure water.

Each rapid increase of the total AE energy visible on the AE curve denotes a crack occurring of in the clay sample at a given moment. As seen in this figure, the biggest cracks were formed in the second stage of the CDRP and in the first stage of FDRP. At this stage the sample surface became dry while the core of the sample was still wet, and material cracks occurred at this stage.

Figure 29 presents comparison of total AE energy for dried clay saturated with water containing different concentration of surfactant SDS (0, 0.001, 0.01, 0.1 and 1%).

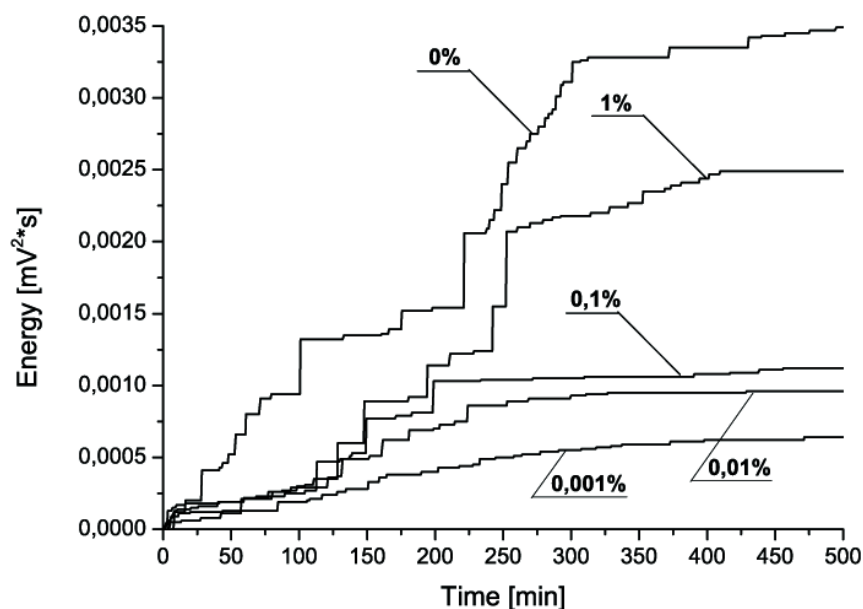


Figure 29. Comparison of total AE energy emitted by clay with different concentration of SDS

It is seen that different amounts of SDS added to water solutions used for clay saturation differentiate the total AE energy emitted by kaolin-clay during drying. As it follows from this figure, the greatest energy is emitted for clay saturated with pure water (0% SDS) and for the greatest surfactant concentration (1% SDS). It means that there is a SDS concentration at which the AE energy reaches minimum. The limit value of the surfactant concentration, at which the drying results are efficient is called *the critical micelle concentration (CMC)*.

Figure 30 shows that the quality of sample with 0.01% surfactant concentration is much better than that with 0% (pure water) concentration.

Figure 30 proves that surfactant concentration of value close the CMC have a meaningful influence on moisture transport inside capillary-porous materials. These conclusion is confirmed by the good quality of dried product visualized on the photo of samples bottom surface presented in figure 30b.

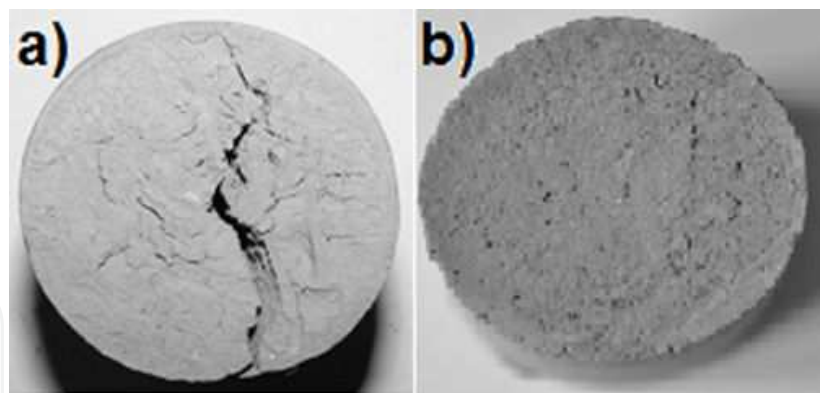


Figure 30. Bottom surface of kaolin-clay samples after drying: a) without surfactant, b) with 0.01% of SDS

7. Conclusions

The presented in this chapter results of research concerning analysis of the AE activity in dried materials allows to state that the AE method can indeed support the control of the drying process and facilitate the guidance for the purpose of avoiding destruction of materials during drying. Comparison of the drying induce stresses simulated numerically on the basis of mechanistic drying model with the experimentally measured descriptors of AE activity reveal an excellent adherence of the theoretical and experimental results. Although with the AE method we are not able to estimate strictly the magnitude of generated stresses, however, the assessment of material destruction intensity caused by the stresses and the time and place of their occurrence is very helpful for control of drying processes. Besides, monitoring of the AE events can be helpful also for validation of the failure criterion formulated on the basis of the mechanistic theory of drying, which is used for estimation of the magnitude and location of maximal stresses as well as their time evolution during drying.

It is worth to point out here the importance of the acoustic emission method that allows us observations *on line* the development of the acoustic signals connected with the destruction of the materials. The possibility of the registration of various descriptors such as: the intensity of acoustic signals, the energy of emitted signals and the total number of signals or total amount of energy allows the current control of drying processes.

Acknowledgements

This work was carried out as a part of research project No. N N209 031638 and N N209 104337 sponsored by the Polish Ministry of Education and Science.

Author details

Stefan Jan Kowalski*, Jacek Banaszak and Kinga Rajewska

*Address all correspondence to: stefan.j.kowalski@put.poznan.pl

Poznań University of Technology, Institute of Technology and Chemical Engineering, Department of Process Engineering, Poznań, Poland

References

- [1] Berlinsky, Y. M, Rosen, J, & Simmons, J. Wadley HNG, ((1990). A Calibration Approach to Acoustic Emission Energy Measurement, *Journal of Nondestructive Evaluation*, 10 (1).
- [2] Banaszak, J, & Kowalski, S. J. (2002). Drying induced stresses estimated on the base of elastic and viscoelastic models. *Chem Eng J* , 86, 139-143.
- [3] Banaszak, J, & Kowalski, S. J. (2010). *Acoustic methods in Engineering Applications*, Publisher: Poznań University of Technology, Poznań (in Polish).
- [4] Banaszak, J, & Kowalski, S. J. (2005). Theoretical and experimental analysis of stresses and fractures in clay like materials during drying, *Chem. Engineering and Processing*, , 44, 497-503.
- [5] Cottrell, A. H. (1970). *The mechanical properties of matter*. Warsaw: PWN (in Polish).
- [6] Kowalski, S. J. (2002). Theoretical study of stress reversal phenomena in drying of porous media. *Dev. Chem. Eng. Mineral Process.*, 10(3/4): 261-280.
- [7] Kowalski, S. J. (2003). *Thermomechanics of Drying Processes*, Springer, Berlin, Heidelberg.
- [8] Kowalski, S. J. (2010). Control of mechanical processes in drying. Theory and Experiment, *Chemical Engineering Science*, , 65, 890-899.
- [9] Kowalski, S. J, Banaszak, J, & Rybicki, A. (2012). Damage Analysis of Microwave-Dried Materials, *AIChE Journal*.
- [10] Kowalski, S. J, & Musielak, G. (1999). Deformations and stresses in dried wood. *Transport in Porous Media* , 34, 239-248.
- [11] Kowalski, S. J, Molinski, W, & Musielak, G. (2004). Identification of fracture in dried wood based on theoretical modeling and acoustic emission. *Wood Sci Technol* , 38, 35-52.
- [12] Kowalski, S. J, & Pawlowski, A. (2010). Drying of wet materials in intermittent conditions,, *Drying Technol.* 28 (5). , 636-643.

- [13] Kowalski, S. J, & Rajewska, K. (2002). Dried induced stresses in elastic and viscoelastic saturated materials. *Chem Eng Sci* , 57, 3883-3892.
- [14] Kowalski, S. J, Rajewska, K, & Rybicki, A. (2000). Destruction of wet materials by drying, *Chem. Eng. Sci.* , 55, 6755-6762.
- [15] Kowalski, S. J, & Rybicki, A. (1996). Drying stress formation induced by inhomogeneous moisture and temperature distribution. *Transport in Porous Media* , 24, 139-156.
- [16] Kowalski, S. J, & Rybicki, A. (2007). The vapour-liquid interface and stresses in dried bodies, *Transport in Porous Media* , 66, 43-58.
- [17] Luong Phong M(1994). Centrifuge simulation of Rayleigh waves in soils using a drop-ball arrangement, *ASTM Special Technical Publication*, (1213), 385-399.
- [18] Malecki, I, & Ranachowski, J. (1994). *Acoustic emission: Sources, Methods Applications*, Pascal Publications, Warszawa (in Polish).
- [19] Mujumdar, A. S. Ed.) ((2007). *Handbook of Industrial Drying (Third Edition)*, Taylor & Francis Group, New York.
- [20] Strumiłło Cz(1983). *Fundamentals of the Theory and the Technology of Drying*, WNT Warszawa, (in Polish).
- [21] Wert, C. A, & Thomson, R. M. (1974). *Physics of solids*, National Scientific Publishers, London, UK